

Enhancement of Nanocomposite for Humidity Sensor Application

N. D. Md Sin, Mohamad Fadzil Tahar, M. H. Mamat and M. Rusop

Abstract This chapter investigates the improvement of nanocomposited ZnO/SnO₂ that was prepared on ZnO coated glass using thermal chemical vapor deposition (CVD). The sensor properties were characterized using current-voltage (*I*–*V*) measurement (Keithley 2400). The results analyzed were for ZnO agglomerate nanoparticle, SnO₂ nanorod, and ZnO/SnO₂ composite nanorods. The structural properties were characterized using field emission scanning electron microscopy (FESEM) (JEOL JSM 6701F). The thin films were tested using two-point probe and the sensors characterized using *I*–*V* measurement (Keithley 2400) in a clean humidity chamber (ESPEC SH-261). The chamber was set at the same room temperature (25 °C) with percent relative humidity (RH%) varied in the range of 40–90%RH. ZnO/SnO₂ composite nanorods performed the highest sensitivity with 265 ratio compared to the ZnO agglomerate nanoparticle and SnO₂ nanorod. The response and recovery time for ZnO/SnO₂ composite nanorods were 227 s and 34 s respectively.

1 Introduction

Humidity sensors have been important for the precise control and reliable estimate of water vapors content in atmospheres from industrial processes to the general improvement in the quality of life [1, 2]. Generally a humidity sensor has to possess fast response and recovery time, high sensitivity, good stability, negligible

N. D. Md Sin (✉) · M. F. Tahar · M. H. Mamat · M. Rusop
Faculty of Electrical Engineering, NANO-ElecTronic Centre (NET),
40450 Shah Alam, Selangor, Malaysia
e-mail: nordiyana86@yahoo.com

M. Rusop
NANO-Scitech Centre (NST), Institute of Science, Universiti Teknologi MARA (UiTM),
40450 Shah Alam, Selangor, Malaysia

hysteresis over periods of usage, and possibly a large operating range for both humidity and temperature [3]. As an *n*-type wide bandgap semiconductor ($E_g = 3.6$ eV) tin dioxide (SnO_2) nanostructures having rutile structure attracted great interest in recent years. SnO_2 has good characteristics in optical, electrical, chemical, and thermal stability [4]. ZnO is one of the most important group of II–VI semiconductor materials. It is an *n*-type and a wide bandgap material with a direct bandgap (3.37 eV) and large excitation binding energy of 60 MeV. ZnO also comes from Wurtzite-structured semiconductors that can help to mix with SnO_2 [5]. Zinc and tin compounds have recently attracted considerable attention because they display technological properties [6], such as high capacity anode material, which can also be used for oxygen separation acting as a photo catalyst under the visible light, humidity and gas sensors action [7, 8]. Doping is an attractive and effective method for manipulating various applications of semiconductors.

Using single materials can cause low sensitivity of sensor [9] due to the insufficient exposing surface area and low electron transportation due to the surface morphology. This is because nanogenerators, sensors, and piezoelectric tubes based on nanostructures strongly depend on the strength and stiffness of the materials [10]. Combining ZnO and SnO_2 on thin film can produce high sensitivity due to the heterogeneous interfaces between them.

Sensitivity, selectivity, response time, recovery time, and stability can be improved by combining different additives to SnO_2 [11]. Composite type sensors were suggested to improve thermal reliability because they contain many heterogeneous boundaries between different phases [12, 13]. For example ZnO/CuO, SnO_2 /CuO, SnO_2 /ZnO composites showed increased sensitivities in comparison to single-phase materials [14, 15]. Composites are beneficial because the combination of materials tend to be more porous. Especially, SnO_2 can be made more porous with addition of small amount of ZnO [16]. This porosity may play an imperative role in humidity sensing because the pores of the materials serve as adsorption sites. The sensitivity of the sensor directly depends on these pore sizes.

In this chapter, we introduce the technique of chemical vapor deposition method to prepare ZnO/ SnO_2 composite nanorod on a glass substrates cover with ZnO thin film for humidity sensor applications. This technical paper investigates the effect of nanocomposited ZnO/ SnO_2 on the surface morphology and humidity sensor application. The growth mechanism of ZnO/ SnO_2 composite nanorod has been discussed.

2 Methodology

The glass substrates were cleaned with acetone, methanol, and deionized water in the ultrasonic device using several steps before the experiment began. At first, ZnO thin film was deposited on glass substrates using the radio frequency (RF) magnetron sputtering method. ZnO coated glass were deposited (high purity (99.999 %)) on glass substrate using RF magnetron system at RF power 200 W.

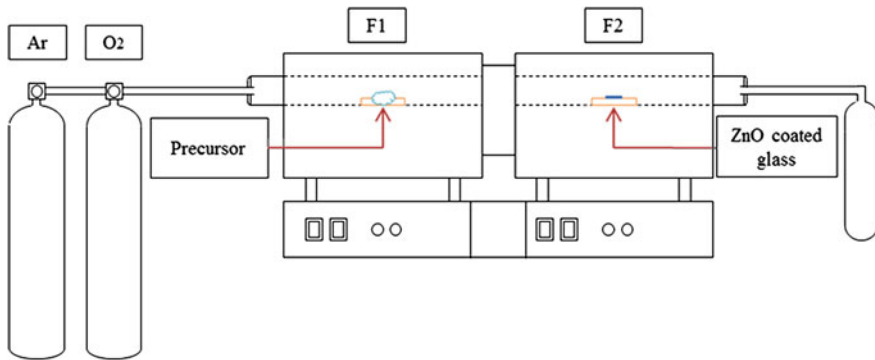


Fig. 1 CVD process

The pressure of the system was maintained at 7 m Torr and the sputter chamber was pumped at 5×10^{-4} Pa using a molecular pump. The gases were injected into the chamber with ratio of flow rate argon to oxygen (45:5) sccm. The ZnO thin films were deposited for 60 min with substrate temperature 500 °C.

In the second process, these ZnO films act as the template for ZnO/SnO₂ composite nanorod deposition. Two furnaces were used to grow doped ZnO/SnO₂ composite nanorods thin film as shown in Fig. 1. Furnace 1 was used to place precursor and Furnace 2 was used to place ZnO coated glass. Both precursor and glasses use a single Quartz tube. Zinc nitrate and tin chloride act as the precursor, Argon (Ar) as the carrier gas, and oxygen (O₂) as the reactor gas. The flow rates of the gases were 20 sccm for Ar and 5 sccm for O₂. Both precursors were measured with 3 g. The substrate temperature was deposited at 500 °C and the deposition time was set at 1 h.

The humidity sensor measurement was conducted on Au metal contact deposited on the thin film as the electrode using thermal evaporation. The thin films were tested using two-point probe and the sensor was characterized using *I*-*V* measurement system (Keithley 2400) in a clean humidity chamber (ESPEC SH-261). The chamber had been set at the same room temperature (25 °C) with percent relative humidity (RH%) varied in the range of 40–90%RH. Structural properties were characterized using FESEM (JEOL JSM 6701F). Then the *I*-*V* was plotted using the Leios TMXpert software.

3 Result and Discussion

3.1 Structural Properties

Figure 2a shows the FESEM image of nanoparticle of ZnO template at 30,000 times magnification. The size of nanoparticle is in range of 75–85 nm. This ZnO template acts as a holder for ion zinc in thermal CVD method. The FESEM image at

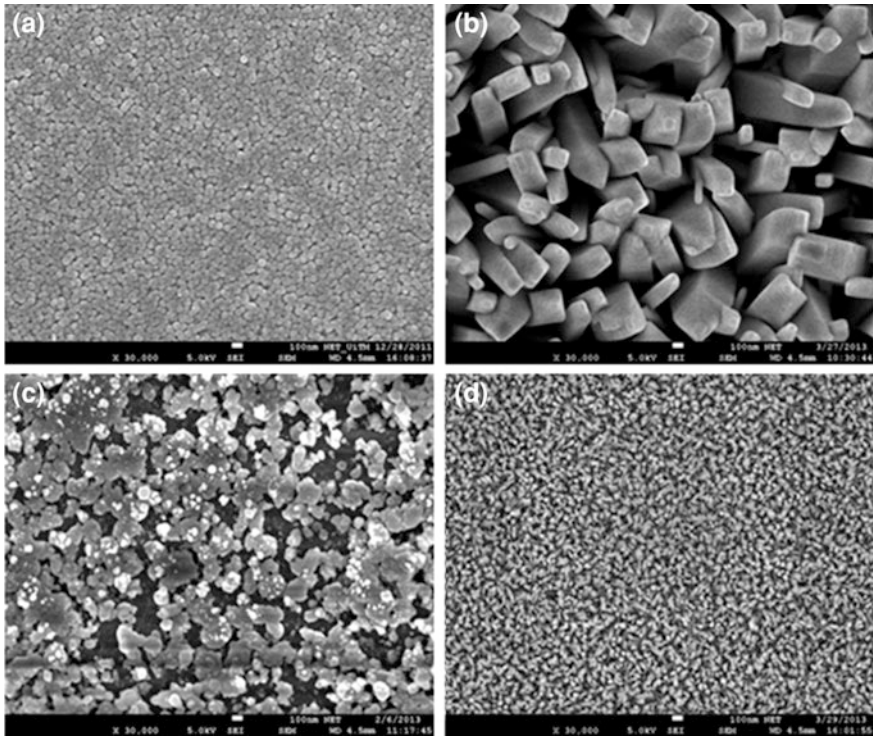
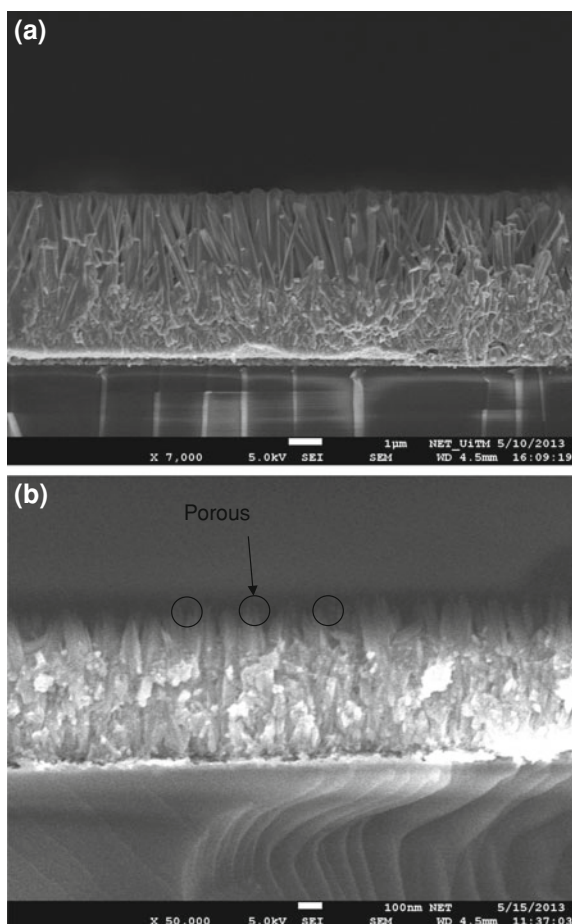


Fig. 2 FESEM images for **a** ZnO template **b** ZnO nanoparticle **c** SnO₂ nanorod and **d** ZnO/SnO₂ composite nanorods at magnification 30 kx

30 K magnification, as shown in Fig. 2b–d, shows the SnO₂ nanorods, ZnO agglomerate particle, and ZnO/SnO₂ composite nanorods. The surface images show that all films are uniformly deposited on ZnO template layer. The size of tip of SnO₂ nanorods was around 80–110 nm while the size of ZnO/SnO₂ composite nanorods was in the range of 35–50 nm. From the surface image, the size of nanorod of ZnO/SnO₂ composite nanorods reduces compared with SnO₂ nanorods as shown in Fig. 2c and d. This reduction of size enhances the high surface area that can increase the sensitivity because of larger site area to absorb the water vapor [17, 18, 19]. Besides, Fig. 3a and b shows the cross-sectional view of the SnO₂ nanorods and ZnO/SnO₂ composite nanorods respectively. The image shows the growth of well-aligned SnO₂ nanorods and ZnO/SnO₂ composite nanorods on ZnO template. It can be observed that the thickness of the SnO₂ nanorods is on average 5.4 μ m. The thickness of ZnO/SnO₂ composite nanorods was on average 840 nm. The growth of SnO₂ nanorods on ZnO template for humidity sensor is come newly in this study. The growth of aligned SnO₂ nanorods is promoted by ZnO template as shown in Fig. 3a. Although it is hard to grow the SnO₂ nanorods on ZnO template since both materials are not in the same lattice group of structure, it is still possible for growth due to homogeneous nucleation [20, 21]. Salehi et al. [22] fabricated

Fig. 3 The cross-sectional view of **a** SnO_2 nanorods and **b** ZnO/SnO_2 composite nanorods



SnO_2 pore structure-based gas sensor deposit on glass substrate using chemical vapor deposition method and SnCl_4 as the precursor. Based on the ZnO/SnO_2 composite nanorods cross-sectional view, a porous structure is observed, as indicated in Fig. 3b, that promotes improvement in sensor performance [23–25]. Compared to other findings, Wang et al. [26] prepared Zn_2SnO_4 nanowire using thermal evaporation method by heating Sn and Zn powder as the precursor without any catalyst with diameter thickness of 50 nm. The use of two precursor of ZnO and SnO_2 deposit on ZnO template became a novelty in this study.

Table 1 shows the atomic percent for all the samples, refer to the EDS spectrum images in Fig. 4 (a) SnO_2 nanorods (b) ZnO agglomerate particle and (c) ZnO/SnO_2 composite nanorods. Table 1 and Fig. 4 show the possible corresponding chemical composition. It reveals that zinc (Zn), oxygen (O), and tin (Sn) are the

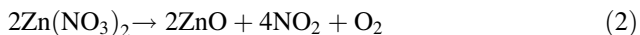
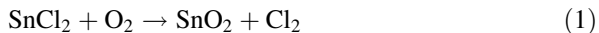
Table 1 Atomic percent of ZnO nanoparticle, SnO₂ nanorod, and ZnO/SnO₂ composite nanorods thin films

Atomic percent (%)	Zn	Sn	Si	O	C
SnO ₂	0	28.47	5.28	66.26	0
ZnO	11.32	0	20.72	62.89	5.07
ZnO/SnO ₂	0.87	71.59	3.75	23.79	0

constituent parts of ZnO/SnO₂ composite nanorods. The EDS measurements show that the dominant compositions for ZnO/SnO₂ composite nanorods thin film are Zn (0.87 %), Sn (71.59 %), and O (23.79 %).

The XRD patterns of SnO₂ nanorods, ZnO agglomerate particle, and ZnO/SnO₂ composite nanorods show polycrystalline as depicted in Fig. 5. The diffraction of SnO₂ nanorods contained diffraction peaks from tetragonal SnO₂ (JCPDS card no. 41-1445). While the ZnO agglomerate particle match with hexagonal wurzite ZnO (JCPDS card no. 36-1451). ZnO/SnO₂ composite nanorods diffraction peaks can be indexed with the tetragonal SnO₂ and hexagonal wurzite ZnO. It is observed that the peaks of SnO₂ nanorods reveal at diffraction peaks (101) (211) (002) (301). The higher intensity is at (101) and (002) of SnO₂ compared to other peaks. This indicates that SnO₂ nanorods enhance to the (002) peak that are preferably orientated in [001] direction [27, 28]. The diffraction peak of ZnO agglomerate particle depict at (100) (002) (101) (102) (110), and (103). However, ZnO/SnO₂ composite nanorods perform peak of ZnO at (100) orientation whereby the dominant peaks belong to tetragonal SnO₂ show at peaks (110) (101) (211) (002), and (301). The (100) peaks of ZnO indicate that the ZnO precursor acts as the holder to the ZnO/SnO₂ composite nanorods.

The possible growth of ZnO/SnO₂ composite nanorods is discussed as indicated in Fig. 6. In this study, no metal catalyst has been used. The growth of ZnO/SnO₂ composite nanorods was influenced with ZnO thin film that acts as the template layer. The growth mechanism can be understood based on vapor solid growth (VS) process. The chemical reaction can be explained as:



SnCl₄ and Zn(NO₃)₂ were reduced to Sn and Zn vapor by reaction at 500 °C. The source SnCl₄ and Zn were carried by the flowing Ar gas and react with O₂ gas (Eqs. (1) and (2)). The Zn was directly deposited on the ZnO template. Then the ZnO templates act as the nucleation sites for the growth of ZnO nanostructures. Once the initial nucleation starts, the crystal grows in epitaxial ways, which results in the preferential orientation of ZnO/SnO₂ composite nanorods in the end.

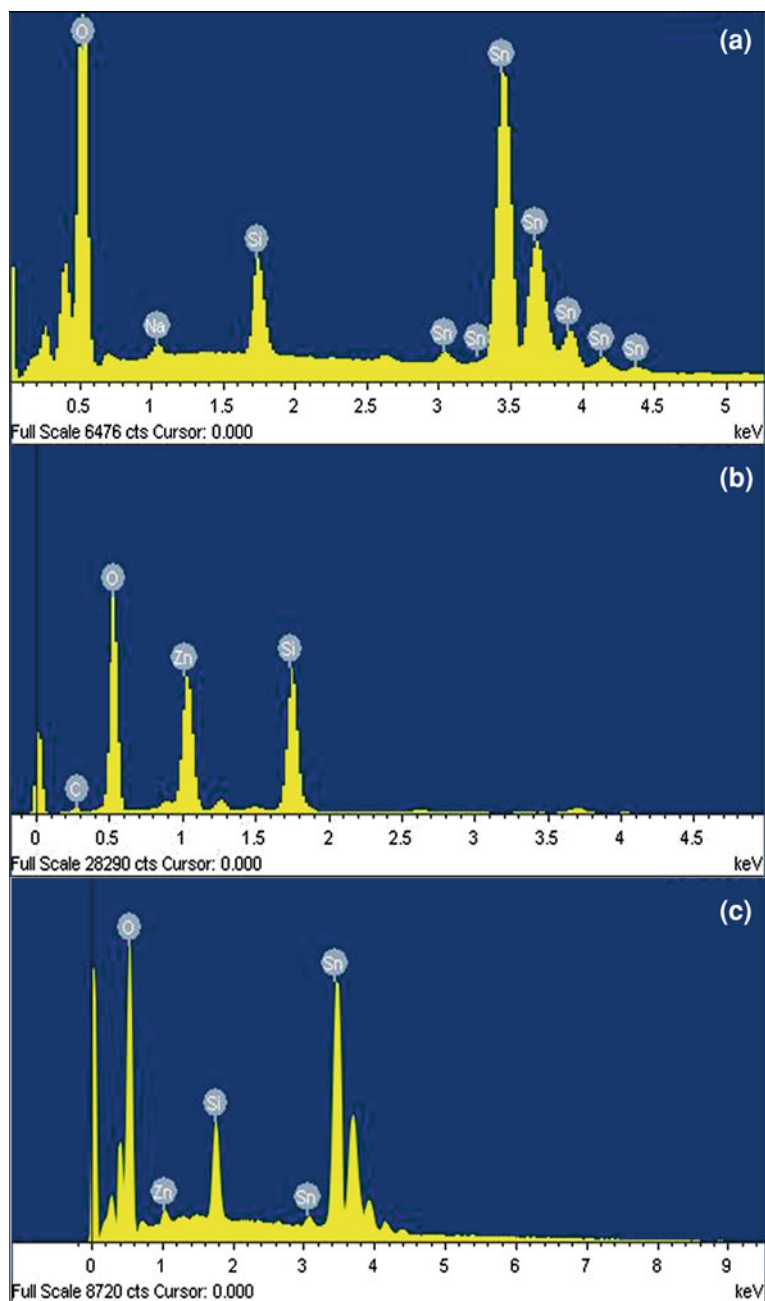


Fig. 4 EDS spectrum images for **a** ZnO nanoparticle, **b** SnO₂ nanorod, and **c** ZnO/SnO₂ composite nanorod thin films

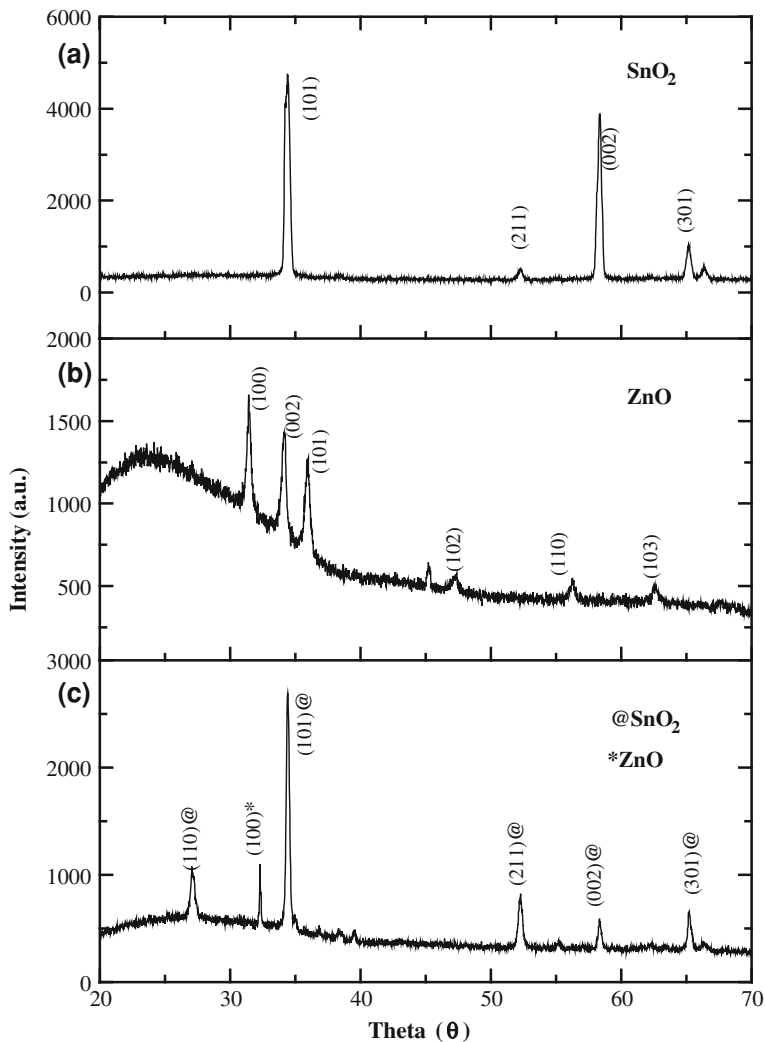


Fig. 5 The XRD pattern of **a** SnO_2 nanorods, **b** ZnO nanoparticle, and **c** ZnO/SnO_2 composite nanorods

3.2 Optical Properties

Figure 7 shows PL spectra of (a) SnO_2 nanorods (b) ZnO agglomerate nanoparticle, and (c) ZnO/SnO_2 composite nanorods excited by He-cd laser operating at 325 nm. The SnO_2 nanorods show a broad peak at around 630 nm as the ZnO agglomerate nanoparticle and ZnO/SnO_2 composite nanorods depict two emission bands at ultraviolet (UV) emission and broad visible region. The UV emission and

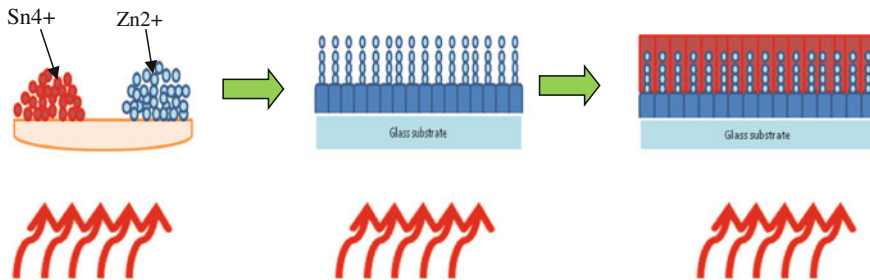


Fig. 6 The possible growth mechanism of ZnO/SnO₂ composite nanorods on ZnO template

visible region of ZnO agglomerate nanoparticle is indicated at around 400 nm and 650 nm, respectively, while the ZnO/SnO₂ composite nanorod signifies at around 380 nm and 585 nm respectively. Both samples show a weak peak at UV region and a dominant peak at visible area. The UV emission corresponds to the recombination of free excitons of ZnO [29]. The visible peak corresponds to existence of the Zn and Sn interstitial defect, oxygen vacancies in ZnO and SnO₂, and residual strain tempt during the growth process. These prominence peaks may contribute to better interaction between the adsorbed water vapor and the active layer [30]. From the graph, the peaks of ZnO/SnO₂ composite nanorods move to the left (blue shift) from the peaks of ZnO agglomerate nanoparticle and SnO₂ nanorods. The blue shift can be explained due to the transition of electron transition, mediated by oxygen vacancies [31]. The high intensity level of ZnO/SnO₂ composite nanorods was high compared with ZnO agglomerate nanoparticle and SnO₂ nanorods. It may contribute by the rougher surface of ZnO/SnO₂ composite nanorods.

3.3 Humidity Sensor Fabrication

Figure 8a–c shows *I*–*V* plots for thin films for ZnO nanoparticle, SnO₂ nanorod, and ZnO/SnO₂ composite nanorods with relative humidity of 40–90 % at 25 °C. The samples were given supplied voltage from –5 to 5 V. The current increases when relative humidity increases so the resistance is decreased. This is because the water vapor on the surface of thin films was absorption. This water vapor can increase the flow of the current through the thin film with less resistance. The water vapor in air has a strong influence on the conductivity of the thin films [32]. In any RH atmosphere, *I*–*V* curves of the device exhibit good linear behavior, which proves a good ohmic contact between the surfaces and Au electrodes.

The composite ZnO/SnO₂ composite nanorods sensor exhibited significantly higher sensitivity than sensor constructed solely from ZnO nanoparticle or SnO₂ nanorod itself due to the heterogeneous interfaces between them and more adsorption site was created that can help more water vapor to be absorbed [16].

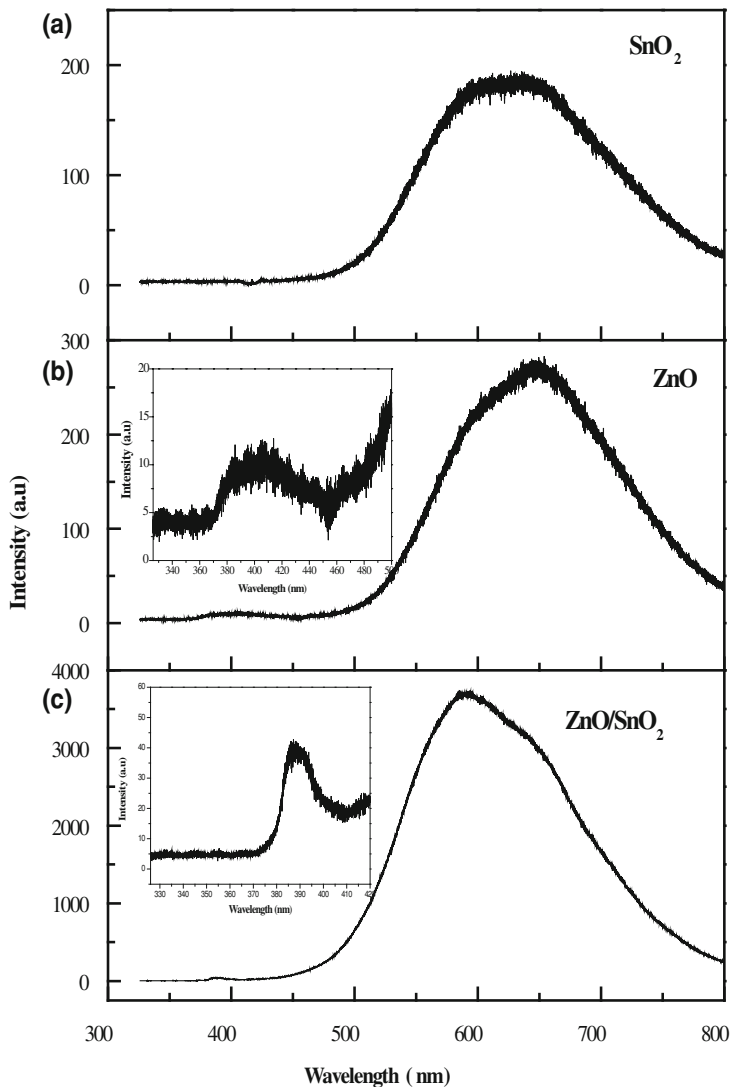


Fig. 7 Photoluminescence spectra **a** SnO_2 nanorods, **b** ZnO agglomerate nanoparticle, and **c** ZnO/SnO_2 composite nanorods

The graph in Fig. 8 shows that sensitivity increases when RH increases. This phenomenon is related to water adsorption on the thin films. At low RH, water adsorbing on the surfaces will not donate electrons to sensing layers and will significantly lower the sensitivity of thin films. The larger the surface area, the larger the content of water adsorbed, so the density of charge carrier becomes larger and hence the sensitivity increases [33]. The sensing mechanism is based on the absorption and desorption process between the surface structure and humidity [34].

Fig. 8 **a** I - V measurement at different RH% of Md Sin SnO₂ nanorods, **b** ZnO nanoparticle, and **c** ZnO/SnO₂ composite nanorods

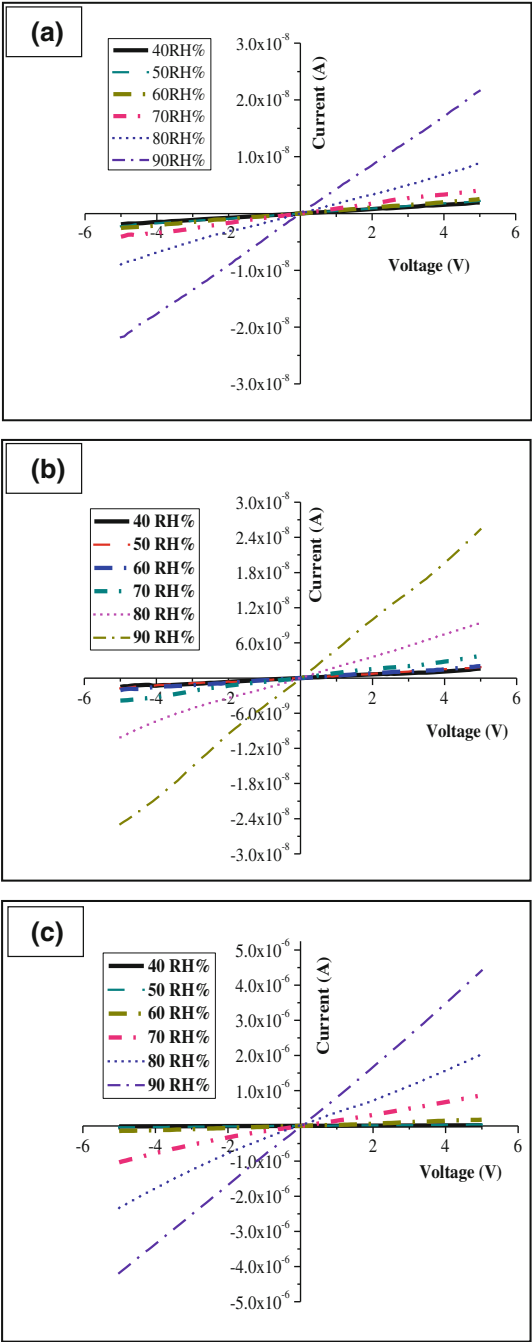


Table 2 The value of sensitivity and response and recovery times of SnO₂ nanorods, ZnO agglomerate nanoparticle and ZnO/SnO₂ composite nanorods are summarized

Sample (ZnO/SnO ₂)	Sensitivity	Response (s)	Recovery (s)
SnO ₂	16	371	114
ZnO	11	392	259
ZnO/SnO ₂	265	227	34

For sensitivity, the value was calculated using Eq. (3) [35]:

$$S = \frac{I_{90\text{RH}\%}}{I_{40\text{RH}\%}} \quad (3)$$

where S as sensitivity, $I_{40\text{RH}\%}$ as current of the sensor in dry condition, and $I_{90\text{RH}\%}$ as current at 90RH% (relative humidity). The sensitivity values are listed in Table 2. The sensor current of SnO₂ nanorods and ZnO agglomerate nanoparticle at 40%RH were 1.94×10^{-9} A and 1.61×10^{-9} A respectively. Whereas at 90%RH, the current of SnO₂ nanorods and ZnO agglomerate nanoparticle was 2.16×10^{-8} A and 2.54×10^{-8} A respectively. The changes in current are based on the equation performed 11 and 16 times for SnO₂ nanorods and ZnO agglomerate nanoparticle respectively. The changes in current at about two orders at 40%RH is 1.67×10^{-8} A is 265 times than 90%RH is 4.42×10^{-6} A of ZnO/SnO₂ composite nanorods. From Table 1, the ZnO/SnO₂ composite nanorods sensor exhibited significantly higher sensitivity than sensor constructed solely from ZnO agglomerate nanoparticle and SnO₂ nanorod itself due to the heterogeneous interfaces between them and more adsorption site was created that could help more water vapor to be absorbed [16]. Besides, the high surface area facilitates the reaction with water vapor and sensing layer of ZnO/SnO₂ composite nanorods sensor [36, 37]. Moreover, the advantage of one-dimensional structure (1D) of ZnO/SnO₂ composite nanorods sensor could assist the electron to transverse along the rods' structure [37].

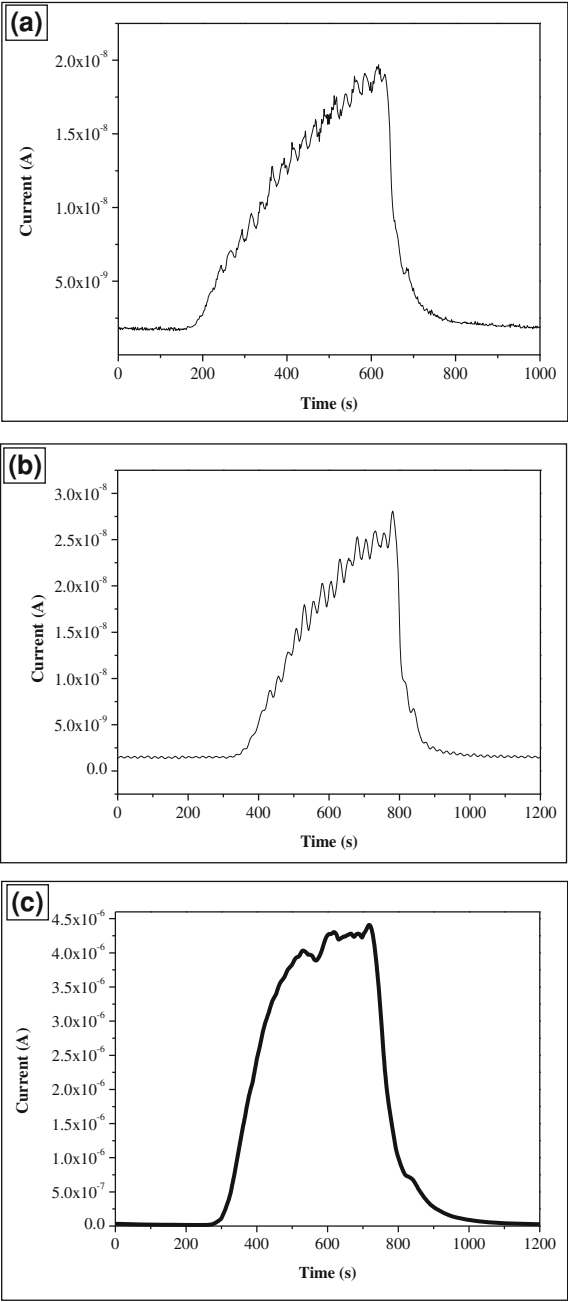
Figure 9 shows the response and recovery time of (a) SnO₂ nanorods, (b) ZnO agglomerate nanoparticle, and (c) ZnO/SnO₂ composite nanorods with the time taken for the transition total current to become constant from 40 to 90%RH (adsorption process) is assigned as response time and 90 to 40%RH (desorption process) for the recovery time. The sensor was given bias 5 V. Table 1 shows the calculated response and recovery time using Eq. (4) [38]:

$$I(t) = I_0 \left(1 - e \left(-\frac{t}{t_r} \right) \right) \quad \text{for the response time (absorption process)} \quad (4)$$

$$I(t) = I_0 e \left(-\frac{t}{t_d} \right) \quad \text{for the recovery time (desorption process)}$$

where I is the magnitude of current, I_0 is saturated current, t is time, t_r is response time constant, and t_d is the recovery time constant. When the thin films were

Fig. 9 The response and recovery characteristics curve of **a** SnO₂ nanorods, **b** ZnO nanoparticle, and **c** ZnO/SnO₂ composite nanorods obtained by changing the RH% between 40 and 90



exposed to the 90%RH, the current through the sensors increased. When the thin films switched to dry condition again (40%RH), the current decreased and reached a relatively stable value. According to Table 2, the response times of the SnO₂ nanorods and ZnO agglomerate nanoparticles were 371 s and 392 s, respectively, while the recovery time of the SnO₂ nanorods and ZnO agglomerate nanoparticles were 114 s and 259 s respectively. ZnO/SnO₂ composite nanorod has the fastest time to response and recovery time with 227 s and 34 s respectively.

The sensing mechanism is based on the absorption and desorption process between the surface structure and humidity [34]. At low humidity, the tips and defects of the thin films present a high local charge density and a strong electrostatic field, which promotes water dissociation. The dissociation provides protons as charge carriers of the hopping transport [39]. At high humidity, one or several serial water layers are formed among thin films, and electrolytic conduction between sensing materials takes place along with photonic transport and becomes dominating in the transport process [39].

4 Conclusion

In this chapter, ZnO/SnO₂ composite nanorods were successfully synthesized using thermal CVD. The SnO₂ nanorods, ZnO agglomerate nanoparticle, and ZnO/SnO₂ nanoflower were successfully grown on ZnO template layer. The SnO₂ nanorod and ZnO agglomerate nanoparticles produce sensitivity with 16 and 11 ratios of times. The ZnO/SnO₂ composite nanorods give the highest sensitivity with ratio of 265 times. The response and recovery time for these ZnO/SnO₂ composite nanorods are the fastest among ZnO nanoparticles and SnO₂ nanorods with 227 s and 34 s respectively.

References

1. Pelino, M., Cantalini, C., Faccio, M.: Principles and applications of ceramic humidity sensors. *Act. Passiv. Elect. Compon.* **16** (1994)
2. Shimizu, Y., Yamazoe, N.: Humidity Sensors: Principles and Applications. *Sens. Actuators* **10**, 379–398 (1986)
3. Regtien, P.P.L.: Humidity sensors. *Meas. Sci. Technol.* **23**(1) (2012)
4. Z. Chen CL (2005). Humidity sensors: a review of materials and mechanisms, *Sens*
5. Z.L. Wang ZCK (1998) Functional and Smart Materials Structural Evolution and Structure Analysis
6. Wang, C., Wang, X., Zhao, J., Mai, B., Sheng, G., Peng, P., Fu, J.: Synthesis, characterization and photocatalytic property of nano-sized Zn₂SnO₄. *J. Mater. Sci.* **37**, 2898–2996, (2002)
7. Young, D.L., Williamson, D.L., Coutts, T.J.: Structural characterization of zinc stannate thin films. *J. Appl. Phys.* **91**, 1464 (2002)

8. Stambolova, I., Konstantinov, K., Kovacheva, D., Peshev, P., Donchev, T.: Spray pyrolysis preparation and humidity sensing characteristics of spinel zinc Stan-nate thin films. *J. Solid State Chem.* **128**, 5 (1997)
9. Zhu, C.L., Chen, Y.J., Wang, R.X., Wang, L.J., Cao, M.S., Shi, X.L.: Synthesis and enhanced ethanol sensing properties of α -Fe₂O₃/ZnO heteronanostructures. *Sens. Actuat.* **140**, 185–189 (2009)
10. Yu GJXZD: Effect of surface morphology on the mechanical properties of ZnO nanowires (2010)
11. Chengxiang Wang, L.Y., Luyuan, Z., Dong, X., Rui, G.: *Sensors. Metal Oxide Gas Sensors: Sensitivity and Influencing Factors* (2010)
12. De Lacy Costello, B.P.J., Ewen, R.J., Jones, P.R.H., Ratcliffe, N.M., Wat, R.K.M.: A study of the catalytic and vapour-sensing properties of zinc oxide and tin dioxide in relation to 1-butanol and dimethyldisulphide. *Sens. Actuat. B* **61**, 199–207 (1999)
13. Yu, J.H., Choi, G.M.: Electrical and CO gas sensing properties of ZnO–SnO₂ composites. *Sens. Actuat. B* **52**, 251–256 (1998)
14. Moon, W.J., Yu, J.H., Choi, G.M.: Selective CO gas detection of SnO₂–Zn₂SnO₄ composite gas sensor. *Sens. Actuators B* **80**, 21–27 (2001)
15. Zhang YSSaTS: Preparation, structure and gas-sensing properties of ultramicro ZnSnO₃ powder. *Sensors and Actuators B* **12**, 5–9 (1993)
16. Wagh LAP, M.S., Seth, T., Amalnerkar, D.P.: Surface cupricated SnO₂–ZnO thick film as a H₂S gas sensor. *Mater. Chem. Phys.* **84**, 228–233 (2004)
17. Jamil, H., Batool, S.S., Imran, Z., Usman, M., Rafiq, M.A., Willander, M., Hassan, M.M.: Electrospun titanium dioxide nanofiber humidity sensors with high sensitivity. *Ceram. Int.* **38**(3), 2437–2441 (2012)
18. Kuang, Q., Lao, C., Wang, Z.L., Xie, Z., Zheng, L.: High-sensitivity humidity sensor Based ON a single SnO₂ nanowire. *J. Am. Chem. Soc.* **129**(19), 6070–6071 (2007). doi:[10.1021/ja070788m](https://doi.org/10.1021/ja070788m)
19. Song, X., Qi, Q., Zhang, T., Wang, C.: A humidity sensor based on KCl-doped SnO₂ nanofibers. *Sens. Actuators B: Chem* **138**(1), 368–373 (2009)
20. Feder, J., Russell, K., Lothe, J., Pound, G.: Homogeneous nucleation and growth of droplets in vapours. *Adv. Phys.* **15**(57), 111–178 (1966)
21. Oxtoby, D.W.: Homogeneous nucleation: theory and experiment. *J. Phys.: Condens. Matter* **4**(38), 7627 (1992)
22. Salehi, A.: A highly sensitive self heated SnO₂ carbon monoxide sensor. *Sens. Actuators B: Chem.* **96**(1–2), 88–93
23. Kim, H., Sathaye, S.D., Hwang, Y.K., Jung, S.H., Hwang, J., Kwon, S.H., Park, S., Chang, J.: Humidity sensing properties of nanoporous TiO₂–SnO₂ ceramic sensors. *Bull. Korean Chem. Soc.* **26**(11), 1881 (2005)
24. Wang, W., Tian, Y., Li, X., Wang, X., He, H., Xu, Y., He, C.: Enhanced ethanol sensing properties of Zn-doped SnO₂ porous hollow microspheres. *Appl. Surf. Sci.* (2012)
25. Yuan, Q., Li, N., Tu, J., Li, X., Wang, R., Zhang, T., Shao, C.: Preparation and humidity sensitive property of mesoporous ZnO–SiO₂ composite. *Sens. Actuators B: Chem.* **149**(2), 413–419 (2010)
26. Wang, L., Zhang, X., Liao, X., Yang, W.: A simple method to synthesize single-crystalline Zn₂SnO₄ (ZTO) nanowires and their photoluminescence properties. *Nanotechnology* **16**(12), 2928 (2005)
27. Jiang, Q., Li, Y., Du, G., Liu, Y., Zhao, H.: A novel structure of SnO₂ nanorod arrays synthesized via a hydrothermal method. *Mater. Lett.* **94**, 100–103 (2013)
28. Wang, Y.-L., Guo, M., Zhang, M., Wang, X.-D.: Hydrothermal preparation and photoelectrochemical performance of size-controlled SnO₂ nanorod arrays. *CrystEngComm* **12**(12), 4024–4027 (2010). doi:[10.1039/c0ce00201a](https://doi.org/10.1039/c0ce00201a)
29. Asokan, K., Park, J., Choi, S.-W., Kim, S.: Nanocomposite ZnO–SnO₂ nanofibers synthesized by electrospinning method. *Nanoscale Res. Lett.* **5**(4), 747–752 (2010). doi:[10.1007/s11671-010-9552-y](https://doi.org/10.1007/s11671-010-9552-y)

30. Kannan, P.K., Saraswathi, R., Rayappan, J.B.B.: A highly sensitive humidity sensor based on DC reactive magnetron sputtered zinc oxide thin film. *Sens. Actuators A* **164**(1–2), 8–14 (2010)
31. Wang, Z., Huang, B., Liu, X., Qin, X., Zhang, X., Wei, J., Wang, P., Yao, S., Zhang, Q., Jing, X.: Photoluminescence studies from ZnO nanorod arrays synthesized by hydrothermal method with polyvinyl alcohol as surfactant. *Mater. Lett.* **62**(17), 2637–2639 (2008)
32. Parthibavarman, M., Hariharan, V., Sekar, C.: High-sensitivity humidity sensor based on SnO₂ nanoparticles synthesized by microwave irradiation method. *Mater. Sci. Eng.* **31**, 840–844 (2011)
33. Qin, K., Lao, C., Zhong Lin, W., Xie, Z., Lansun, Z.: High-sensitivity humidity sensor based on a single SnO₂ nanowire (2007)
34. Md Sin, N.D., Mamat, M.H., Musa, M.Z., Abdul Aziz, A., Rusop, M.: Effect of growth duration to the electrical properties of Zn doped SnO₂ thin film toward humidity sensor application (2012)
35. Qi Qia, T.Z., Yi, Z., Haibin, Y.: Sensors and actuators humidity sensing properties of KCl-doped Cu. *Sens. Actuators, B* **137**, 21–26 (2009)
36. Gu, L., Zheng, K., Zhou, Y., Li, J., Mo, X., Patzke, G.R., Chen, G.: Humidity sensors based on ZnO/TiO₂ core/shell nanorod arrays with enhanced sensitivity. *Sens. Actuators B: Chem.* **159**(1), 1–7 (2011)
37. Song, Xiaofeng, Liu, Li: Characterization of electrospun ZnO–SnO₂ nanofibers for ethanol sensor. *Sens. Actuators, A* **154**(1), 175–179 (2009)
38. Mamat, M.H., Khusaimi, Z., Musa, M.Z., Malek, M.F., Rusop, M.: Fabrication of ultraviolet photoconductive sensor using a novel aluminium-doped zinc oxide nanorod–nanoflake network thin film prepared via ultrasonic-assisted sol–gel and immersion methods. *Sens. Actuators, A* **171**(2), 241–247 (2011)
39. Xu, L., Wang, R., Xiao, Q., Zhang, D., Liu, Y.: Micro humidity sensor with high sensitivity and quick response/recovery based on ZnO/TiO₂ composite nanofibers. *Chin. Phys. Lett.* **28**, 070702 (2011)

Recent Trends in Nanotechnology and Materials
Science

Selected Review Papers from the 2013 International
Conference on Manufacturing, Optimization, Industrial
and Material Engineering (MOIME 2013)

Lumban Gaol, F.; Webb, J. (Eds.)

2014, X, 103 p. 66 illus., 7 illus. in color., Hardcover

ISBN: 978-3-319-04515-3